Crystal fields in ErCu, ErAg, and ErZn†

P. Morin and J. Pierre
Laboratoire de Magnétisme, Centre National de la Recherche Scientifique, B.P. 166, 38042-Grenoble-Cedex, France

J. Rossat-Mignod
Departement de Recherche Fondamentale-D.N., Centre d'Etudes Nucléaires, B.P. 85, 38041-Grenoble-Cedex, France

K. Knorr* and W. Drexel
Institut Laüe-Langevin, B.P. 156, 38042-Grenoble-Cedex, France

(Received 4 February 1974)

The splitting of the crystal-field levels in the intermetallic compounds ErM (M = Ag, Cu, Zn) has been determined by inelastic neutron scattering experiments. In all three cases, the crystal-field parameters $A_4^0\langle r^4\rangle$ and $A_6^0\langle r^6\rangle$ are negative and of the same order of magnitude. The ground state is always a $\Gamma_8^{(3)}$ quadruplet. The point-charge model fails to explain the large values of the sixth-order terms. The crystal-field Hamiltonian interprets well the magnetic properties of these compounds.

I. INTRODUCTION

The equiatomic compounds of the heavy lanthanides with mono- and divalent metals like Cu, Ag, and Zn are cubic (CsCl structure).

Magnetization measurements on single crystals of the heavy-rare-earth–zinc compounds revealed ferromagnetic behavior.[1] The effects of the crystalline electric field (CEF) on the direction and the value of the magnetic moment in the ordered state were considered to be important. Point-charge estimates, however, did not give a satisfactory explanation of the observed results. In addition, the analysis of these measurements is difficult because the crystal field might lower the symmetry of the ordered phase by the Jahn-Teller effect.[2]

The equiatomic compounds of heavy lanthanides and monovalent metals are antiferromagnets.[3] The magnetic structures of TbCu,[4] DyCu,[5] HoCu,[6] ErCu,[7] TbAg,[4] DyAg,[8] HoAg, and ErAg,[9] have been solved by neutron diffraction. These structures can be described by a propagation vector of $q=(\frac{1}{2},\frac{1}{2},0)$. The direction of the moments could be explained by crystal-field effects.[5,6] Magnetic susceptibility might give a further insight into these effects. For CeAg, e.g., the fourth-order term of the crystal field was derived from this type of measurement.[6]

The most direct determination of the crystal field, however, can be achieved by neutron spectroscopy. So far, two results on rare-earth intermetallics with CsCl structure exist. Brun *et al.*[10] worked on PrAg and presented two possible sets of crystal-field parameters. Measurements of Chamard-Bois *et al.*[11] on HoRh showed a very high sixth-order term of the crystal field.

Our aim was to study the crystal-field splitting of the heavy rare-earth compounds with CsCl structure, in particular the compounds with Cu, Ag and Zn, by inelastic neutron scattering. As the magnetic interactions are quite high in these systems, the ErM compounds present the best choice, since here the ordering temperatures are below 20 K (Table III). We reduced the already small magnetic interactions further by diluting Er in Y. In this paper, we will thus present the results of inelastic neutron scattering on the compounds $Er_{0.2}Y_{0.8}Ag$, $Er_{0.2}Y_{0.8}Cu$ and $Er_{0.2}Y_{0.8}Zn$ in the paramagnetic phase.

II. NEUTRON SPECTROSCOPY

Crystal field

Using the nomenclature of Lea *et al.*,[12] the crystal-field Hamiltonian in cubic symmetry can be written, with the quantization axis along the fourfold one:

$$\mathcal{H}=W\left\{\frac{x}{F_4}(O_4^0+5O_4^4)+\frac{1-|x|}{F_6}(O_6^0-21O_6^4)\right\}\ .$$

W is an energy scaling factor and x is a measure of the ratio of fourth- and sixth-order terms. Lea *et al.* have tabulated the eigenvalues and eigenvectors. Their result for the Er^{3+} ion ($J=\frac{15}{2}$) is reproduced in Fig. 1.

The magnetic neutron cross section for a single ion is given by Trammell[13]:

$$\frac{d^2\sigma}{d\Omega d\omega}=C\left(\frac{1.91e^2}{2mc^2}g_J\right)^2F^2(\vec{Q})\times\frac{k_f}{k_i}\sum_{n,m}\rho_m|\langle n|\vec{J}_\perp|m\rangle|^2\delta(E_n-E_m-\hbar\omega)\ ,$$

where k_i and k_f are the wave vectors of the ingoing and outgoing neutron, $F(\vec{Q})$ is the form factor, $\vec{J}_\perp$ is the component of the total angular momentum per-

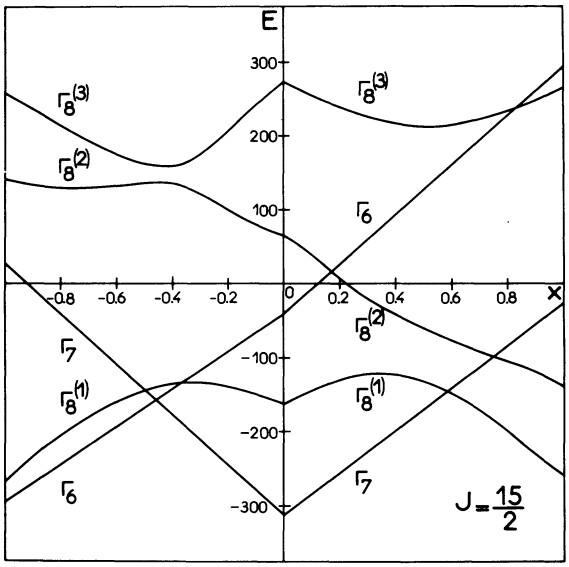

FIG. 1. Crystal-field energy levels in units of W as a function of x after Lea *et al.* (Ref. 12).

pendicular to the scattering vector $\vec{Q}$, and ρ_m is the thermal population of the initial state which obeys to the Boltzmann statistics. Transitions between the states $|n\rangle$ and $|m\rangle$ occur with a matching change in neutron energy $\hbar\omega$. Matrix elements can be calculated in a straightforward manner; for the rare-earth ion in cubic crystal fields, they have been tabulated by Birgeneau.[14]

Experimental methods

The samples were prepared by melting the elements with an induction furnace, in alumina crucibles for Cu and Ag and in sealed tantalum crucibles for Zn compounds. In order to obtain a good homogeneity, they are remelted and quenched. They showed a single phase in x-ray investigations. One hundred grams of the polycrystalline samples were placed in a cryostat which allowed measurements between liquid helium and room temperatures.

The experiments were performed on the statistical chopper time-of-flight spectrometer IN7 at the Institut Laüe-Langevin. The incident energy E_i was 33.41 meV, the counting times ranged from 15 to 24 h. An array of nine detectors covered angles between 19° and 21° which was before the first Bragg reflection. All spectra were dominated by a very intense elastic line, whose width never exceeded the instrumental resolution of seven channels (full width at half-maximum; this corresponds to 2.0 meV at 33.41 meV) as determined separately by a measurement of vanadium. The scattering of data points is determined visually from the otherwise flat background. One should keep in mind that the spectra produced by the statistical chopper are not directly physical, but the result of a correlation process. The consequence is that the absolute error is the same for each time-of-flight channel, independent of the actual number of counts in this channel. At the right-hand side of the elastic line upward transitions are induced while the neutron is losing energy; at the left-hand side the neutron is gaining energy by deexcitation processes.

One additional measurement on $Er_{0.2}Y_{0.8}Zn$ at room temperature was carried out on the rotating crystal time-of-flight spectrometer IN4 ($E_i = 42.30$ meV). Since here nearly one-half of the scattering plane was covered with detectors, we were able to study the q dependence of the observed inelastic structures. The fact that these structures vanished at higher scattering angles, the absence of any inelastic structure in YZn and finally the temperature dependences found, confirmed that we had to deal with crystal-field transitions.

III. RESULTS

In addition to the elastic peak, well-resolved structures have been observed which in the following will be explained as transitions between CEF levels of the Er^{3+} ion in cubic symmetry. For each sample, the first experiment was always undertaken at low temperatures, where only excitation processes from the ground levels are possible. At higher temperatures one expects additional transitions from excited levels on the energy-gain as well as on the energy-loss sides.

ErAg compound

The spectra obtained on $Er_{0.2}Y_{0.8}Ag$ at 9 and 51 K are given in Fig. 2. At 9 K two excitation peaks at 5.0 and 11.7 meV were observed. From the energy transfers and the ratio of the intensities, these peaks can be unambiguously associated to transitions from a $\Gamma_8^{(3)}$ ground state to Γ_6 and $\Gamma_8^{(2)}$ excited states, respectively, which gives a value of x of about $+0.42$. The widths were slightly larger than the experimental resolution. The second temperature (51 K) was chosen in order to populate the Γ_6 excited level; in addition to the former excitation peaks a deexcitation peak was observed corresponding to the $\Gamma_6 \rightarrow \Gamma_8^{(3)}$ transition, but no additional excitation processes from Γ_6 were visible.

ErCu compound

The spectra at 7 and 125 K for $Er_{0.2}Y_{0.8}Cu$ are shown in Fig. 3. At 7 K, two excitation peaks at 8.4 and 14.2 meV were observed. They are associated with $\Gamma_8^{(3)} \rightarrow \Gamma_6$ and $\Gamma_8^{(3)} \rightarrow \Gamma_8^{(2)}$ transitions at about $x = +0.34$. The widths exceeded the experi-

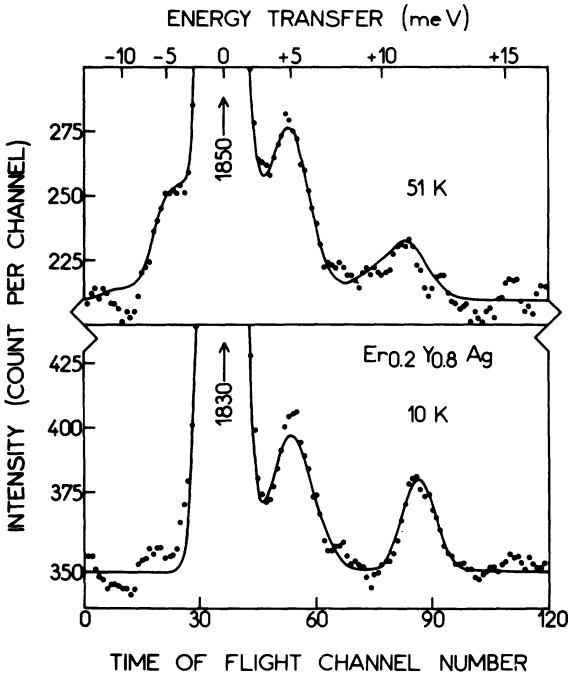

FIG. 2. Neutron energy spectra of $Er_{0.2}Y_{0.8}Ag$. The theoretical spectra are drawn in solid lines.

mental resolution. At 125 K, the populations of the Γ_6 and $\Gamma_8^{(2)}$ excited levels are significant and a new excitation process appeared near 5.2 meV corresponding mainly to the two transitions $\Gamma_8^{(2)} \rightarrow \Gamma_8^{(1)}$ and $\Gamma_8^{(1)} \rightarrow \Gamma_7$. The intensity of the former peaks decreased simultaneously. Two definite deexcitation peaks were observed at about -5 and -14 meV corresponding to $\Gamma_8^{(1)} \rightarrow \Gamma_8^{(2)}$ and $\Gamma_8^{(2)} \rightarrow \Gamma_8^{(3)}$ transitions.

ErZn compound

Three spectra at 10, 125, and 290 K were recorded for $Er_{0.2}Y_{0.8}Zn$ on the spectrometer IN7 (see Fig. 4). At 10 K, the excitation spectrum showed only one intense peak at 12.0 meV with a width of 12 channels. This single peak does not allow determination of a level scheme, but it may correspond to a double transition from the $\Gamma_8^{(3)}$ to the Γ_6 and $\Gamma_8^{(2)}$ excited states, which are degenerated for $x = +0.155$. This assumption is confirmed by the spectrum taken at 125 K when we observed two excitation peaks, the former one at 12.0 meV and a new one at 7.7 meV which corresponds to the very intense transitions $\Gamma_8^{(2)} \rightarrow \Gamma_8^{(1)}$ and $\Gamma_6 \rightarrow \Gamma_8^{(1)}$. The two deexcitation peaks at -7.5 and -12.5 meV are related to the $\Gamma_6, \Gamma_8^{(2)} \rightarrow \Gamma_8^{(3)}$ and $\Gamma_8^{(1)} \rightarrow \Gamma_6, \Gamma_8^{(2)}$ downward transitions. The spectrum at room temperature gave slightly smaller energy transfers; the relative intensities were changed according to the Boltzmann factors.

Finally, we have done additional measurements on $Er_{0.2}Y_{0.8}Zn$ and YZn on the spectrometer IN4 at room temperature. As mentioned above, the main interest was to verify that the CEF transitions vanished at high angles. In addition, the smooth and well-defined background of this instrument allowed a very reliable test on the absence of inelastic structures in YZn. The spectra obtained at an angle of 9° are reproduced in Fig. 5. The positions and relative intensities of the CEF transitions of $Er_{0.2}Y_{0.8}Zn$ are in very good agreement with those obtained on IN7 at the same temperature.

IV. DETERMINATION OF CRYSTAL-FIELD PARAMETERS

After this rough determination of the crystal-field level schemes, we tried to describe the results in a more quantitative way. For this purpose we used a fitting program. We want to emphasize however that the fit is not necessary for the identification of transitions and the determination of approximate values of x and W. Besides x and W, the following parameters enter into the fit: the natural width of CEF transitions, the intensity scaling factor C in the formula for the cross section, the background, the height of the elastic line, the instrumental resolution—which can be well approximated by a constant in time, the height and the width of a

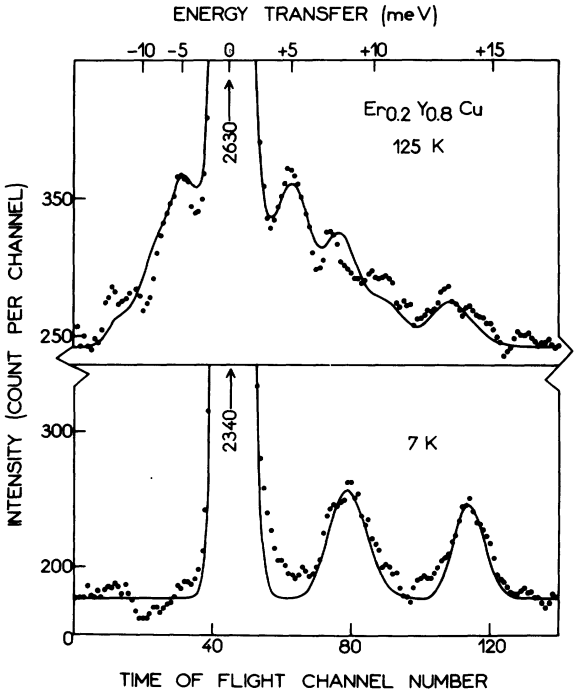

FIG. 3. Neutron energy spectra of $Er_{0.2}Y_{0.8}Cu$.

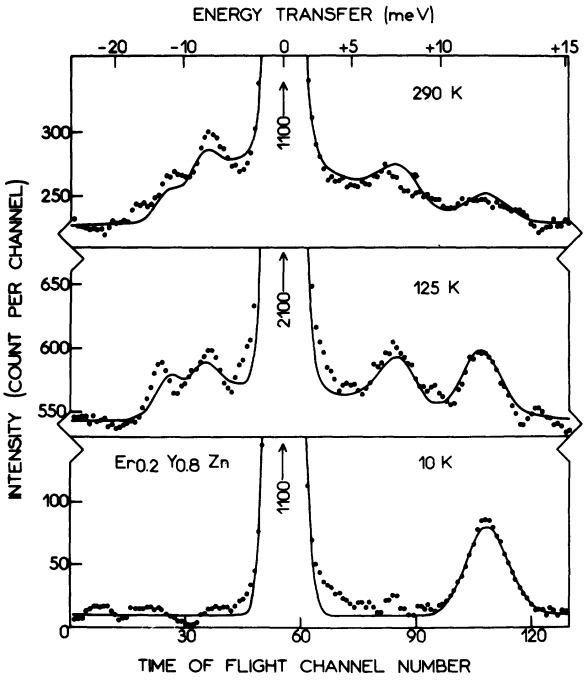

FIG. 4. Neutron energy spectra of $Er_{0.2}Y_{0.8}Zn$ (spectrometer IN7).

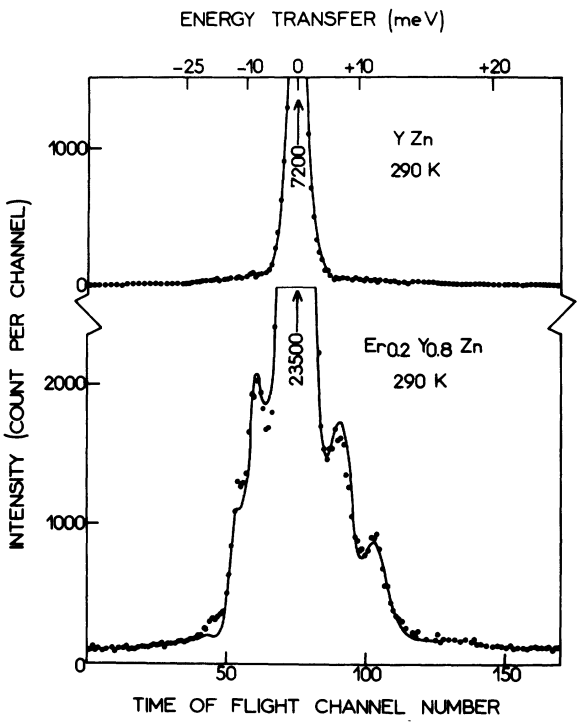

FIG. 5. Neutron energy spectra at room temperature for YZn and $Er_{0.2}Y_{0.8}Zn$ (spectrometer IN4).

quasielastic contribution. All the structures were assumed to be of Gaussian shape. The constant background was always found visually regarding all time-of-flight channels. The physically meaningful parameters resulting from the fit are presented for each spectrum in Table I.

At low temperature, it was not necessary to take into account any quasielastic contribution other than the transitions within CEF levels; for copper and silver compounds, the fit was considerably improved by assuming two different widths for the two observed transitions $\Gamma_8^{(3)} \rightarrow \Gamma_6$, $\Gamma_8^{(3)} \rightarrow \Gamma_8^{(2)}$ [labeled (i) and (ii), respectively in Table I]. Surprisingly the quadruplet-doublet transition was found to be

TABLE I. CEF parameters and line widths deduced from the fitting of the experimental spectra. Values held constant in the fit are underlined.

	T (K)	x	W (meV)	ΔE_t[a] (meV)	ΔE_E[b] (meV)	$A_4^0\langle r^4\rangle$ (meV)	$A_6^0\langle r^6\rangle$ (meV)
$Er_{0.2}Y_{0.8}Ag$	9	+0.425	−0.0442	(i) 2.7 (ii) 1.3	···	−7.05	−0.89
	51	+0.419	−0.0426	<u>1.7</u>	8.7		
$Er_{0.2}Y_{0.8}Cu$	7	+0.342	−0.0565	(i) 2.0 (ii) 1.0	···	−7.25	−1.30
	125	+0.340	−0.0541	<u>1.7</u>	12.7		
$Er_{0.2}Y_{0.8}Zn$	10	+0.158	−0.0524	1.8	···	−3.11	−1.54
	125	+0.166	−0.0518	<u>1.7</u>	13.2		
	290	+0.158	−0.0500	<u>1.7</u>	17.9		

[a]Natural width (full width at half-maximum) of CEF transitions calculated from the experimental line width and the resolution of the spectrometer.

[b]Full width at half-maximum of the quasielastic contribution.

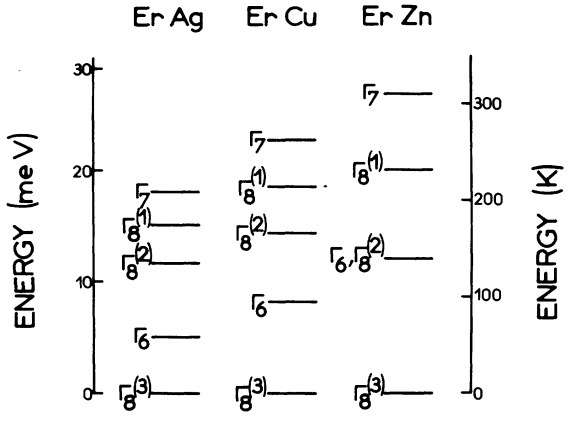

FIG. 6. Crystal-field level scheme in the three compounds.

larger than the quadruplet-quadruplet transition.

At high temperatures, a relatively broad quasielastic contribution appeared. This fact and the decrease of the intensities due to the Boltzmann factor lowered the ratio of the CEF structures to the scattering of data points. Therefore, we found it unreasonable to determine reliable values for the transition widths which were fixed to the mean value of 1.7 meV found at low temperature. The theoretical spectra are shown as solid lines in the figures. In all cases, the average deviation between experimental and calculated spectra was less than the scattering of the data points. However, the transition widths seemed to be slightly overestimated at high temperatures. The values of x and W at low temperatures lead to the crystal-field splittings drawn in Fig. 6. The conventional CEF parameters $A_4^0\langle r^4\rangle$, $A_6^0\langle r^6\rangle$ calculated from x and W are given in Table I.

V. DISCUSSION

Crystal-field parameters

In the following, we will analyze the CEF parameters determined for the three erbium compounds. We observed two main features: the two parameters x and W keep their sign and stay even in a relatively narrow range in spite of the different lattice parameters and electronic valencies of the alloyed metals. The fourth-order term is about the same in the silver (−7.05 meV) and in the copper (−7.25 meV) compounds, but only half as large in the zinc one (−3.11 meV). The sixth-order term decreases from −0.89 meV for ErAg to −1.54 for ErZn. This variation as passing from monovalent to divalent metals may reflect the decrease in valency. In a point-charge model, where the eight first neighbors M and the six next nearest neighbors R of the CsCl-type structure are taken into account, the CEF parameters can be written:

$$A_4^0\langle r^4\rangle = (e^2/a^5)\langle r^4\rangle (0.7987\, Z_M - 0.4375\, Z_R) \quad ,$$

$$A_6^0\langle r^6\rangle = (e^2/a^7)\langle r^6\rangle (0.3041\, Z_M + 0.0469\, Z_R) \quad .$$

Keeping a trivalent charge for the rare-earth and different possible charges for the alloyed metal, the parameters take the values given in Table II. In order to describe approximately the fourth-order term, we had to assume negative charges on copper and silver and a charge close to zero on zinc. With these values however, the sixth-order terms were too small by one order of magnitude. Similar discrepancies between point-charge estimates and experimentally determined CEF parameters have been observed in many ionic compounds[15] and in some intermetallic rare-earth systems studied so far by inelastic neutron scattering.[11,16] This failure of the point-charge model for the sixth-order terms seems to be due not only to a shielding by conduction electrons, but also to a contribution of the ion itself. Calculations of the band structure of these compounds[17] show that the conduction electrons within the atomic sphere of the rare-earth ions are mostly of d character. Thus shielding (or antishielding) of the fourth-order term may be understood, but it is much more difficult to explain the large value of the sixth-order term since this term could be enhanced only by f electrons, which have a small density in the conduction band.

A small decrease of the CEF splitting was observed as the temperature increased. For instance, the $\Gamma_8^{(3)} \rightarrow \Gamma_8^{(2)}$ transition of $Er_{0.2}Y_{0.8}Zn$ changed from 12.0 meV at 10 K to 11.6 meV at 290 K. This variation can be related to the thermal expansion of the lattice parameter.[2]

We will now compare the variation of the CEF parameters within the RAg series; susceptibility measurements on CeAg[6] indicate that the ground state is the Γ_8 quadruplet which was separated by about 360 K from the Γ_7 excited state, leading to a value of −13.6 meV for $A_4^0\langle r^4\rangle$ in agreement with ErAg results.

Brun *et al.*[10] have investigated the CEF splitting in PrAg by neutron spectroscopy; they proposed two solutions: the first one, $W = -0.328$ meV; $x = -0.97$ ($A_4^0\langle r^4\rangle = -7.21$ meV, $A_6^0\langle r^6\rangle = -0.013$

TABLE II. CEF parameters $A_4^0\langle r^4\rangle$, $A_6^0\langle r^6\rangle$ (meV) calculated from a point-charge model, assuming trivalent erbium and given charges Z_M for the alloyed metal.

	ErAg		ErCu		ErZn	
Z_M	$A_4\langle r^4\rangle$	$A_6\langle r^6\rangle$	$A_4\langle r^4\rangle$	$A_6\langle r^6\rangle$	$A_4\langle r^4\rangle$	$A_6\langle r^6\rangle$
0	−2.85	-0.02_4	−3.50	-0.03_3	−3.03	-0.02_7
1	−1.11	-0.07_5	−1.37	−0.10	−1.18	-0.08_1
2					+0.66	-0.13_7

meV) leads to a sixth-order term one order of magnitude too small compared to our results on $Er_{0.2}Y_{0.8}Ag$; however, their second set, $W=-0.43$ meV; $x=-0.8$ ($A_4^0\langle r^4\rangle=-8.0$ meV and $A_6^0\langle r^6\rangle=-1.12$ meV) is in much better agreement with our results.

Comparison with magnetic properties in the ordered range

Above, we have determined the CEF splitting in the dilute erbium alloys. One does not expect the CEF parameters to change in the concentrated compounds. In the ordered range, the exchange field splits the ground-state quadruplet, changes its wave function, increases the magnetic-moment value, and gives rise to a magnetocrystalline energy. We have calculated the energy and the moment of the ground level by diagonalizing simultaneously the exchange and the crystal-field Hamiltonians for the fourfold and the threefold quantization axes. The exchange field is deduced from the ordering temperature Θ using

$$H_{ex}=n\langle M_z\rangle=\frac{3k_B\Theta\langle J_z\rangle}{g\mu_B J(J+1)} \quad ,$$

n being the molecular-field coefficient. The calculated energies and moments are given in Table III. In the three compounds, the energy is lower along the fourfold axis.

The magnetization experiments on a single crystal of ErZn[1] show that the fourfold axis is indeed the easy direction with a magnetization of $6.83\mu_B$ at 4.2 K, in agreement with the calculation. Along the threefold axis the saturation magnetization is only $6.44\mu_B$ compared to the calculated value of $6.60\mu_B$. The anisotropy energy between the $\langle 001\rangle$ and the $\langle 111\rangle$ axis is found experimentally to be 1.8 K compared with 1.3 K. A magnetic field up to 150 kOe, applied along the easy axis, increases the value of the magnetic moment with an experimental susceptibility of 5.7×10^{-6} μ_B/Oe compared to a calculated value of 4.1×10^{-6} μ_B/Oe. This is an effect of the modification of the wave function, approaching the pure $|\frac{15}{2}\rangle$ state under strong field. The magnetic properties of ErZn are thus in good agreement with the obtained level scheme.

TABLE III. Ordering temperatures, calculated moments along fourfold and threefold axes, and calculated energy difference between these axes.

	Θ (K)	μ_{001} (μ_B)	μ_{111} (μ_B)	$E_{100}-E_{111}$ (K)
ErZn	20	6.84	6.60	−1.3
ErCu	16	6.96	6.16	−2.1
ErAg	18	7.38	6.10	−3.2

TABLE IV. Comparison of experimental CEF parameters $a^5A_4^0\langle r^4\rangle$ and $a^7A_6^0\langle r^6\rangle$ in various CsCl-type compounds.

	HoRh	ErAg	ErCu	ErZn
$a^5A_4^0\langle r^4\rangle$ (10^{-38} meV cm^5)	−48.3	−41.1	−34.4	−17.2
$a^7A_6^0\langle r^6\rangle$ (10^{-53} meV cm^7)	−8.0	−6.6	−7.3	−10.6

For the antiferromagnetic compound ErCu, the direction of the moment is also the fourfold axis (c axis of the quadratic magnetic cell: $2a$, $2a$, a).[7] A spin-flop transition is observed in the ordered range[18] which leads to 2 K to an anisotropy energy E_a of 1.5 K:

$$E_a=\tfrac{1}{2}(\chi_\perp-\chi_\parallel)H_c^2 \quad ,$$

in good agreement with the calculation (2.1 K).

The magnetic structure of ErAg has been recently investigated.[9] Below 9.5 K, the magnetic cell is quadratic as previously, the angle between the c axis and the moment was reported to vary from 75° at 4.2 K to 85° at 9 K. Actually the moments should lie in the basal plane. The observed value of the ordered moment is $7.2\mu_B$ at 4.2 K, close to the calculated value ($7.38\mu_B$).

VI. CONCLUSION

In this paper the neutron spectroscopy results and the magnetic properties for the three erbium compounds have been analyzed coherently in terms of the CEF model. The fourth-and sixth-order terms keep the same sign and stay within the same order of magnitude. The sixth-order term is one order of magnitude larger than expected from a point-charge model.

In order to compare now our results with those on isomorphous HoRh[11] we separate off the effects of the lattice parameters. Therefore we present in Table IV the parameters $a^5A_4^0\langle r^4\rangle$ and $a^7A_6^0\langle r^6\rangle$. They decrease moderately from the rhodium to the copper and silver compounds. For ErZn, however, $a^5A_4^0\langle r^4\rangle$ decreases and $a^7A_6^0\langle r^6\rangle$ increases strongly reflecting a significant change in valency. For the rhodium and copper compounds, band calculations[17] show that the d electrons of the alloyed metal lie in the conduction band. These d levels are spread wide in energy, so that they extend over the whole lattice. In the zinc compound the d states of zinc form a narrow band well below the conduction band. Thus these electrons are much more localized aroung the zinc atoms.

With this background we will continue the investigation of CEF parameters in rare-earth compounds with CsCl structure.

†This work is part of the thesis of P. Morin (Archives Originales Centre National de la Recherche Scientifique No. 9323).

*Present address: Physikalisches Institut, Frankfurt-am-Main, Germany.

[1]P. Morin and J. Pierre, Phys. Status Solidi A 17, 479 (1973); Sol. State Commun., 13, 537 (1973).

[2]P. Morin, J. Laforest, J. Pierre, and J. S. Shah, C. R. Acad. Sci. B 277, 353 (1973). P. Morin and J. Pierre, Phys. Status Solidi A 21, 161 (1974).

[3]R. E. Walline and W. E. Wallace, J. Chem. Phys. 41, 3285 (1964); J. Chem. Phys. 42, 604 (1965). J. Pierre and R. Pauthenet, C. R. Acad. Sci. (Paris) 260, 2739 (1965).

[4]J. W. Cable, W. C. Koehler, and E. O. Wollan, Phys. Rev. 136, A240 (1964).

[5]M. Wintenberger, R. Chamard-Bois, M. Belakhovsky, J. Pierre, Phys. Status Solidi B 48, 705 (1971).

[6]J. Pierre, in *Proceedings of the Eighth Rare-Earth Research Conference, Reno, Nevada*, 1970 (U. S. Bureau of Mines, Reno, Nevada, 1970), p. 1020.

[7]W. C. Koehler (private communication).

[8]G. Arnold, N. Nereson, and C. Olsen, J. Chem. Phys. 46, 4041 (1967).

[9]N. Nereson, J. Appl. Phys. 44, 4727 (1973).

[10]T. O. Brun, G. H. Lander, D. L. Price, G. P. Felcher and J. E. Reddy, in Proceedings of the Ninth International Conference on Magnetism, Moscow, 1973 (unpublished).

[11]R. Chamard-Bois, J. Rossat-Mignod, K. Knorr, and W. Drexel, Solid State Commun. 13, 1549 (1973).

[12]K. R. Lea, J. M. Leask, and W. P. Wolf, J. Phys. Chem. Solidi 23, 1381 (1962).

[13]G. T. Trammell, Phys. Rev. 92, 1387 (1953).

[14]R. J. Birgeneau, J. Phys. Chem. Solidi 33, 59 (1972).

[15]M. T. Hutchings and D. K. Ray, Proc. R. Soc., Lond. 81, 663 (1963).

[16]R. J. Birgeneau, E. Bucher, L. Passell, and K. C. Turberfield, Phys. Rev. B 4, 718 (1971).

[17]M. Belakhovsky, J. Pierre, and D. K. Ray, Phys. Rev. B 6, 939 (1972) and Phys. Rev. B (to be published).

[18]J. Pierre, *Proceedings of the International Conference on Rare-Earth Elements*, Paris-Grenoble, 1969, (Centre National de la Recherche Scientifique, 1970), p. 55.